Theoret. Chim. Acta (Berl.) 55, 267–281 (1980)

THEORETICA CHIMICA ACTA


# Ab initio Calculations of Electrostatic Potentials and Deformation Densities for a Series of Choline Ester Model Systems

Helge Johansen and Sten Rettrup

Department of Chemical Physics, The Technical University of Denmark, DTH 301, DK-2800 Lyngby, Denmark

Birthe Jensen

Department of Chemistry BC, The Royal Danish School of Pharmacy, Universitetsparken 2, DK-2100 Copenhagen, Denmark

*Ab initio* LCAO-MO-SCF calculations using a double zeta basis set have been performed for the methyl esters of acetic acid, carbamic acid, methylcarbonic acid, and trifluoracetic acid, in order to model the corresponding choline esters. The systems have been compared by means of population analyses, electron density differences, electrostatic potentials and potential differences. The significance of the electrostatic potential in connection with crystal structure and packing has been studied. The differences in the proton affinity of the compounds have been correlated to differences in the potentials.

**Key words:** *Ab initio* – Choline ester – Electrostatic potentials – Deformation densities.

## 1. Introduction

Much effort has been devoted to theoretical calculations on choline esters, especially with respect to acetylcholine, a natural neurotransmitter, Fig. 1(I). Most of the investigations have been concerned with the torsion angles C—O—C—C and O—C—C—N, and the methods applied have usually been based upon semi-empirical parameters. A comprehensive review has been published by B. Pullman [1]. *Ab initio* calculations using small basis sets have,

0040–5744/80/0055/0267/$03.00

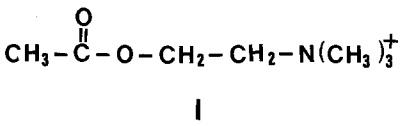

I

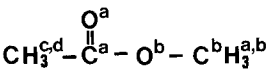

II

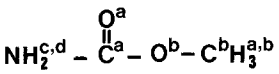

III

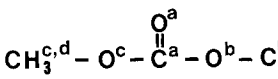

IV

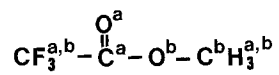

V

**Fig. 1.** Formulae and notations for the considered compounds: I) acetylcholine, II) methylacetate, III) methylcarbamate, IV) dimethylcarbonate, V) methyltrifluoroacetate. Superscripts label atoms which are not related by symmetry

however, been presented [2, 3]. Also the electrostatic potentials have been studied, but only in an INDO framework [4].

The present investigation is not concerned with the torsion angles as such, the PCILO method [1] seems quite able in that respect. Rather, it is a study of the internal and external differences in electronic structures and in electrostatic potentials between various choline esters. The results are to be seen in connection with corresponding crystal structures and may contribute to the understanding of the biological activities of the various compounds.

For this kind of study a basis set of at least double zeta quality was considered necessary, and polarization functions were included for the hydrogen atoms. The esters under consideration are the choline esters of acetic acid, carbamic acid, methylcarbonic acid, and trifluoracetic acid. Also the ester of ethylcarbonic acid was originally included in the calculations, but the results for this compound have been excluded from the paper, as they were essentially identical to those for the methylcarbonic acid ester.

The choline esters were replaced by model systems, Fig. 1(II–V), in which the choline part is simulated by methanol. This is justified since the changes induced through the bonds by the substituents R in R-COO—$(CH_2)$2-$N(CH_3)_3^+$ have died off after the first carbon atom in the alcohol (*vide infra*).

In order to be able to compare the various esters, the geometry for the $-COOCH_3$ part has been fixed and put equal for all systems. It is a valid approximation since minor changes in the geometry are known not to affect the

charge distribution and the potential significantly. Further, the same basis set has been used throughout, whereby basis set errors have been reduced to a minimum.

## 2. Details of Calculations

The coordinates for the four esters considered are given in Table 1. The $-COOCH_3$ geometry is kept fixed, and in order to facilitate the calculations, $C_s$ symmetry (one mirror plane) has been enforced for all the systems. The bond lengths and bond angles have been taken from X-ray structure determinations [5–8], and as the observed differences between the geometries of the different esters hardly are significant, a reasonable average has been used for the COOC part of the molecules.

The calculations in this study are of *ab initio* LCAO-SCF-MO (linear combination of atomic orbitals – self consistent field – molecular orbital) type using the Hartree–Fock–Roothaan formalism [9]. The basis functions are of contracted Gaussian type, and the primitive sets $(X/9, 5)$, $X = C, N, O, F$ and $(H/4)$ reported by van Duijneveldt were used [10]. The notation indicates the number of $s$ and $p$ functions for each atom. For hydrogen the exponents have been scaled by a factor

**Table 1.** Nuclear coordinates in a.u. (1 a.u. $= a_0 = 0.529166 \cdot 10^{-10}$ m). The remaining $H^a$, $H^d$, and $F^b$ coordinates are found by reflection in the symmetry plane $(xy)$. The atomic superscripts are defined in Fig. 1. (The numbers are experimentally significant to at most three places after the decimal point)

| Groups | Atom | $x$ | $y$ | $z$ |
|---|---|---|---|---|
| $-COOCH_3$ | $C^a$ | 0 | 0 | 0 |
| | $C^b$ | 4.430715 | −0.091822 | 0 |
| | $O^a$ | 0 | 2.286464 | 0 |
| | $O^b$ | 2.074189 | −1.452363 | 0 |
| | $H^a$ | 6.010621 | −1.442561 | 0 |
| | $H^b$ | 4.540823 | 1.103199 | 1.697173 |
| $CH_3-$ | C | −2.277839 | −1.654947 | 0 |
| | $H^c$ | −3.990279 | −0.476752 | 0 |
| | $H^d$ | −2.262433 | −2.854931 | 1.697173 |
| $NH_2-$ | N | −2.064902 | −1.445860 | 0 |
| | $H^c$ | −3.799805 | −0.673431 | 0 |
| | $H^d$ | −1.932428 | −3.340322 | 0 |
| $CH_3O-$ | C | −4.423590 | −0.207395 | 0 |
| | $O^c$ | −2.012675 | −1.489301 | 0 |
| | $H^c$ | −5.955392 | −1.612449 | 0 |
| | $H^d$ | −4.575337 | 0.983055 | 1.697173 |
| $CF_3-$ | C | −2.354276 | −1.710482 | 0 |
| | $F^a$ | −4.429442 | −0.282724 | 0 |
| | $F^b$ | −2.335606 | −3.164644 | 2.056665 |

1.3, and a polarization function with exponent 0.8 has been added [11]. The sets have been applied in the contractions $\langle X/4, 2\rangle$ and $\langle H/2, 1\rangle$, respectively.

For the molecular orbital calculations, the joint MOLECULE–ALCHEMY program system [12, 13] was used, and the computations were performed at NEUCC, The Technical University of Denmark.

## 3. Results and Discussion

### *3.1. Population Analysis*

The Mulliken population analysis [14] is not a very accurate tool, but it may be applied when very similar systems are studied using the same basis set. We are especially interested in changes in the $-C^{a}OOCH_3$ part of R-$C^{a}OOCH_3$ as a function of R, since this group seems to be of primary importance in the interaction between the choline esters and the active site of the enzyme acetylcholinesterase, and also because changes in this part may affect the overall conformational pattern of the choline esters.

The results are shown in Table 2. It appears that population changes have died off already at the $CH_3$ group, and the use of model systems, in which the $-CH_2CH_2N(CH_3)_3^+$ chain has been replaced by $-CH_3$, is therefore justified. Also the difference density maps of Sect. 3.2 (Fig. 3) support this approximation.

**Table 2.** Population analysis. q: gross charge, o: overlap population, R: substituent, X: the atom in R which has a bond to $C^a$, $\sigma/\pi$: partition into p and $\pi$ contributions. The atomic superscripts are defined in Fig. 1

| | *R* | | | |
|---|---|---|---|---|
| | $CH_3-$ | $NH_2-$ | $CH_3O-$ | $CF_3-$ |
| $q(C^a)$ | 0.47 | 0.55 | 0.64 | 0.42 |
| $\sigma/\pi$ | 0.18/0.29 | 0.28/0.27 | 0.36/0.28 | 0.19/0.23 |
| $q(O^a)$ | −0.39 | −0.44 | −0.42 | −0.31 |
| $\sigma/\pi$ | 0.07/−0.46 | 0.12/−0.56 | 0.11/−0.53 | 0.08/−0.39 |
| $q(O^b)$ | −0.48 | −0.49 | −0.45 | −0.47 |
| $q(C^b)$ | 0.09 | 0.10 | 0.08 | 0.09 |
| $q(H^a)$ | 0.08 | 0.07 | 0.08 | 0.10 |
| q(X) | −0.22 | −0.46 | −0.44 | 0.73 |
| q(R) | 0.07 | 0.04 | −0.10 | −0.02 |
| $o(C^a-O^a)$ | 1.34 | 1.37 | 1.34 | 1.34 |
| $\sigma/\pi$ | 0.94/0.39 | 1.02/0.35 | 0.99/0.35 | 0.94/0.40 |
| $o(C^a-O^b)$ | 0.52 | 0.61 | 0.63 | 0.55 |
| $\sigma/\pi$ | 0.43/0.09 | 0.55/0.06 | 0.56/0.07 | 0.47/0.08 |
| $o(O^b-C^b)$ | 0.44 | 0.44 | 0.47 | 0.43 |
| $o(C^b-H^a)$ | 0.79 | 0.78 | 0.79 | 0.80 |
| $o(X-C^a)$ | 0.70 | 0.73 | 0.63 | 0.58 |

The results for the gross charges of the acetylcholine analogue ($R = CH_3$) are qualitatively in accord with the results of the STO-3G study [2] for acetylcholine, but the present results tend to be more polarized. The changes as a function of R are rather small. These results for esters are in full agreement with the results of calculations concerning the protonation of carbonyl compounds [15], where it was found that changes in electron distribution caused by replacement of a second hydrogen atom by a hetero atom are smaller than those caused by the first replacement of a hydrogen atom. Among the gross atomic charges $q(C^a)$ and $q(X)$ vary the most. The largest effect on $q(C^a)$ is found for the methylcarbonic acid ester, while the largest effect on $q(X)$ as expected is found for $R = CF_3$. The change in the charge for the carbon atom, by going from $R = CH_3$ to $R = CF_3$, is almost a full electron, but at the same time the group as a whole changes only by 0.1 unit and in the opposite direction. For $C^a$, the rearrangements seem to occur in the $\sigma$ electrons and for $O^a$ primarily in the $\pi$ electrons.

The overlap populations in the bonds of the $-COOCH_3$ group are fairly independent of R, the $C^a-O^b$ bond exhibits the only major change. A certain redistribution of $\sigma$ and $\pi$ character is, however, encountered again.

The change in charge and overlap population are presumably of importance for the hydrolysis of the esters, enzyme catalyzed or simply in aqueous solution. Acetylcholinesterase is known to be acylated by acetylcholine and later rapidly deacylated. By carbamoylcholine the enzyme is again acylated, but deacylation is in this case very slow. Methoxycarbonylcholine and ethoxycarbonylcholine seem to be unable to acylate the enzyme although the affinity for the active site of the enzyme is high [16]. In aqueous solution all of the esters are hydrolyzed more or less rapidly under acid as well as basic conditions, but the detailed mechanisms are not fully known, and kinetic results indicate [17, 18] that different mechanisms apply for different esters. A redistribution of atomic and overlap charges in connection with an attack on the carbonyl carbon atom is, however, for all esters believed to be an essential link in the hydrolysis, and the speed and the pathway of the reaction may depend more on the polarizability than on the charge of the isolated molecule.

Differences in $pK_a$ values of the acids are not reflected in differences in charge distribution of the esters. Also here the ability to undergo charge redistribution on cleavage of the bond $O^b-C^b$ (or in the acids the bond $O^b-H$) must be essential.

### *3.2. Difference Density Maps*

A more detailed picture of the electron density distribution and redistribution as a function of R may be obtained by contour maps of electron density differences. Such maps may also be compared directly with experimentally determined density maps, as found by a combination of X-ray and neutron diffraction measurements (X–N maps). The correspondence is good if the experiment is accurate and if the basis set is of the present quality or better [19]. The populations, on the other hand, cannot be observed, and they are therefore less useful as characteristic features.

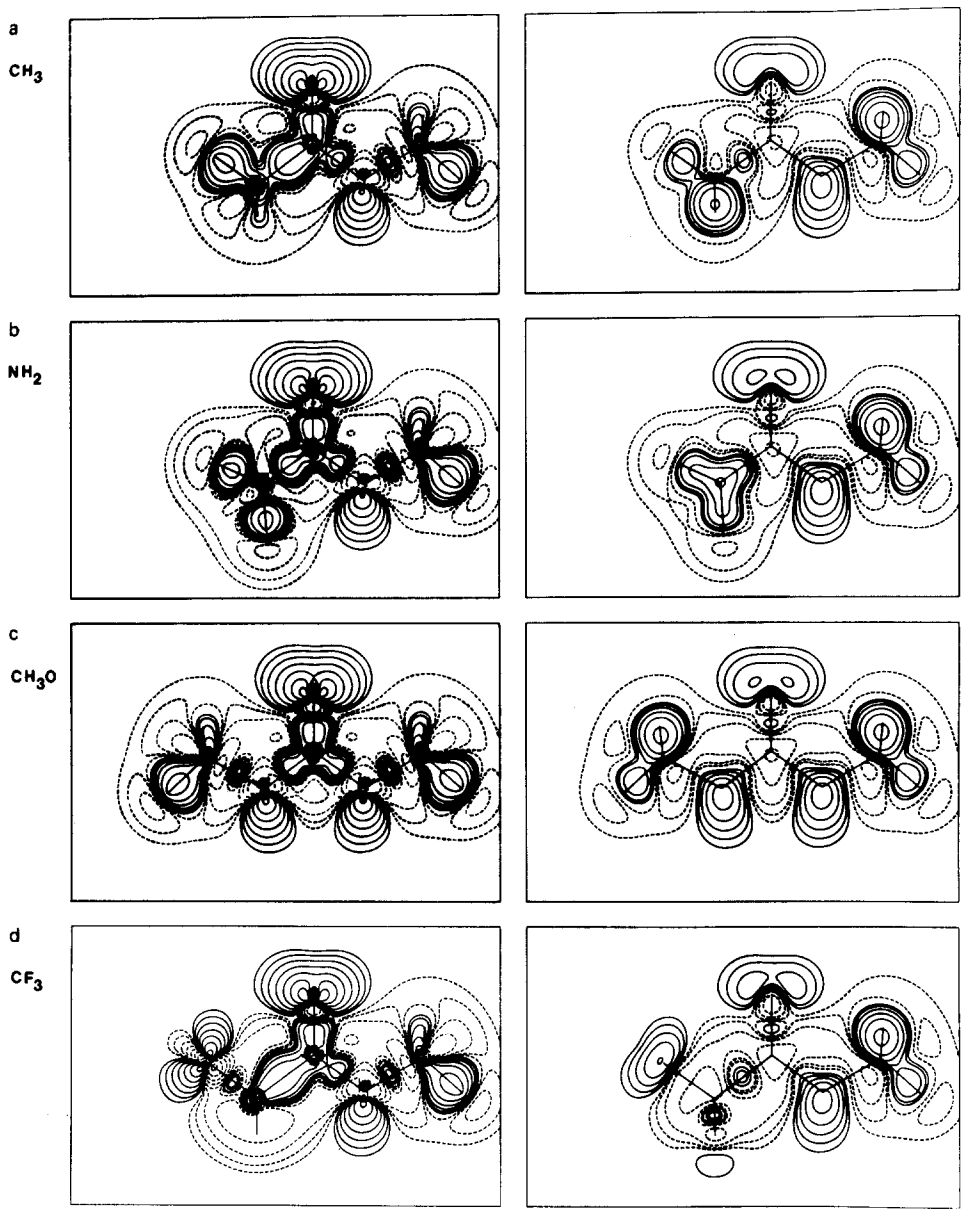


**Fig. 2.** Deformation densities for systems II to V (Fig. 1). Left column depicts densities in the $xy$-plane, right column a plane 1 $a_0$ above. Dashed lines indicate regions with drain of electron density, fully drawn lines indicate accumulation. First contours are $\pm 0.0025 e a_0^{-3}$; neighbouring contours differ by a factor of 2

Fig. 2 shows the so-called deformation density for the four considered molecules, calculated as the difference between the density of the system in question and a superposition of spherically averaged densities for the constituent atoms calculated with the same contracted basis set (not including the polarization

functions). The deformation densities have been depicted in the $xy$-plane, and in a plane 1 $a_0$ above. A certain separation into $\sigma$ and $\pi$ regions is thereby attained.

In the left column of Fig. 2, the $\sigma$ bonds are easily recognized, and so are the lone-pairs on $O^a$, $F^a$, and $O^b$. The density is as usual donated from the outer regions of the molecules. In the right column, the predominant features are the tops of the $O^a$ lone-pairs, the $O^b$ $\pi$ type lone-pair, and bond densities for those $\sigma$ bonds which are not in the $xy$-plane ($C—H^{b,d}$ and $C—F^b$). Only very little density which could be assigned to $\pi$ bonding is found, but this is not unusual.

The maps in Fig. 2 are probably not very informative with respect to the reactivities and structures of these compounds. They have been presented here due to the increasing interest in such maps, especially from experimental quarters. The compounds contain many chemically interesting groups ($CH_3$, $CF_3$, C=O,

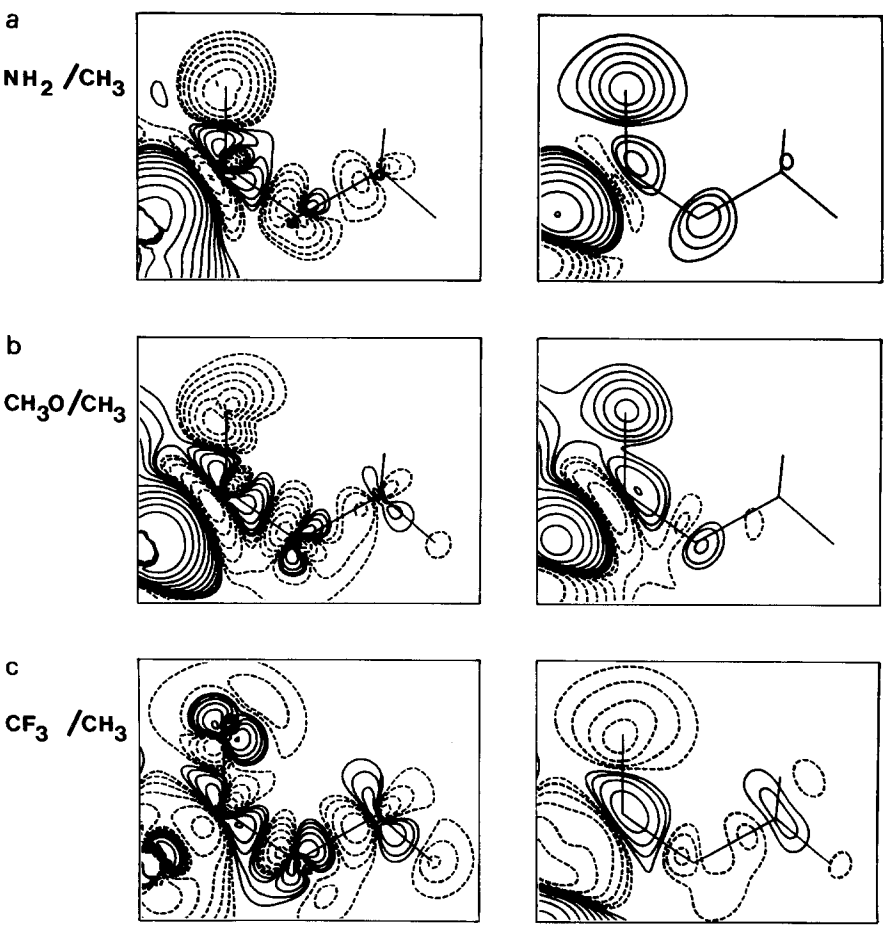


**Fig. 3.** Difference densities for systems III to V (Fig. 1) relative to system II. Planes and lines as in Fig. 2. First contours are $\pm 0.000625 e a_0^{-3}$; neighbouring contours differ by a factor of 2

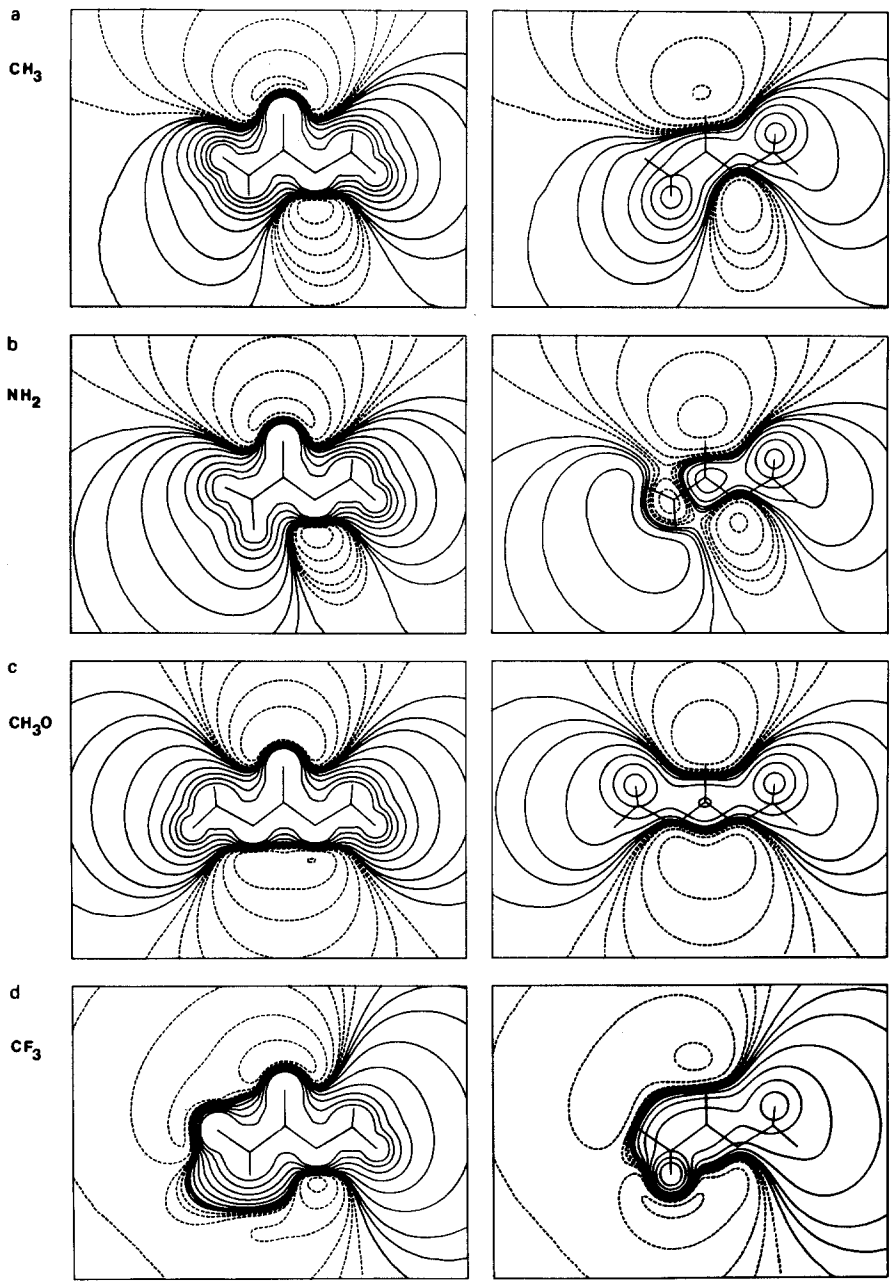


**Fig. 4.** Electrostatic potentials for systems II to V (Fig. 1). Left column depicts potentials in the $xy$-plane, right column a plane 3 $a_0$ above. Dashed lines indicate negative regions. First contours are ±1 kcal/mol; neighbouring contours differ by a factor of 2

C—O), all treated on an equal basis, and the maps show that there is a high degree of transferability with respect to the gross features of deformation densities.

In order to illustrate more subtle changes in the electronic structure of the molecules, molecular difference densities have been depicted in Fig. 3. As molecular reference system the acetylcholine model system ($R = CH_3$) was applied, the purpose being to correlate changes in the electron density for the $-COOCH_3$ region (relative to that of acetylcholine) with activity and reactivity. It should be noted that the features in the lower left corner of the maps in Fig. 3 are meaningless, since different groups are located in that region of space. The contours start at very low values ($\pm 0.0006 e a_0^{-3}$), and the figure therefore illustrates, as mentioned above, that the density changes have virtually died off at the $CH_3$ group.

With $NH_2$ and $CH_3O$ as substituents (Fig. 3a, b), the dominant features are the increase of density in the $\pi$ region of $O^a$ and the decrease in the $\sigma$ region of the same atom. The effects of the two substituents are almost identical. A similar, but less pronounced trend is seen at $O^b$. For $CF_3$ (Fig. 3c) the picture is more or less reversed, and the $\pi$ region of $O^a$ shows a large deficiency compared with the reference molecule. These differences may be important for the affinities of the esters to the active site of acetylcholinesterase and to the different kinds of acetylcholine receptors.

### *3.3. Electrostatic Potential Maps*

Valuable information concerning recognition and reactivity may be obtained from maps of the electrostatic potential for a molecule. In pharmacological literature such a map is sometimes designated an "interaction pharmacophore". Also the packing of molecules and ions in crystals may be understood and in some cases predicted from the electrostatic potentials of the participating units.

The maps depict the potential energy of a positive point-charge by the use of iso-potential contours. Negative potential regions (dashed lines) thus correspond to regions of attraction for positive charge. The energies are, however, only approximative, since polarizability effects have not been considered.

In the present investigation, the electrostatic potentials of the systems II–V, Fig. 1, have been calculated for the isolated molecules, Fig. 4. A word of warning is appropriate at this point. The corresponding choline esters contain a quaternary ammonium group, and since the potentials are of a long-range nature, only the R—COO region will exhibit a reasonable simulation. A further problem arises in the crystals, where the potentials should be combined with the potentials from the negative counter ions (like $Cl^-$, $Br^-$ etc.).

Fig. 4 shows the electrostatic potentials for the four systems. They have been depicted in the $xy$-plane and in a plane 3 $a_0$ above. Negative regions are found around the $O^a$ and $O^b$ lone-pairs as well as in a region around the fluorine atoms. The map in Fig. 4a is in good qualitative agreement with the corresponding map from a semi-empirical calculation on acetylcholine [4], Fig. 6.

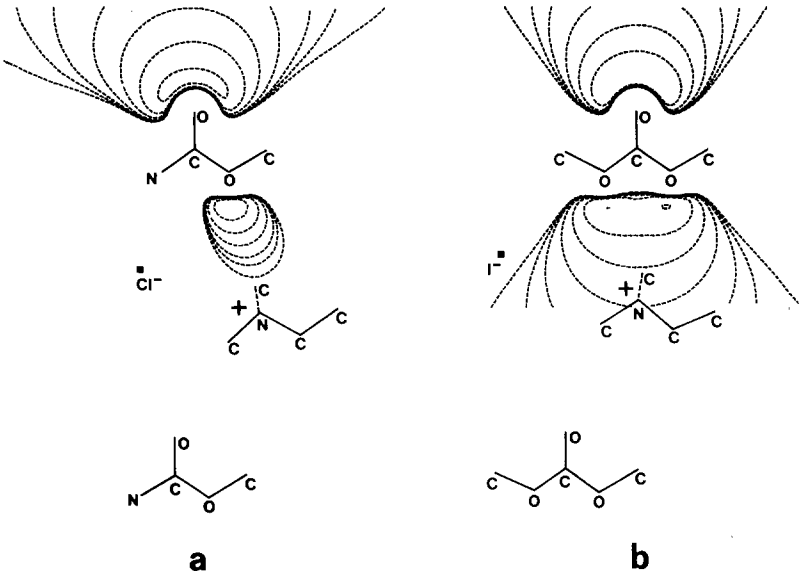


**Fig. 5.** The position of the quaternary ammonium group in carbamoylcholine chloride (a) and methoxycarbonylcholine iodide (b). The regions of negative electrostatic potential (cf. Fig. 4) are shown

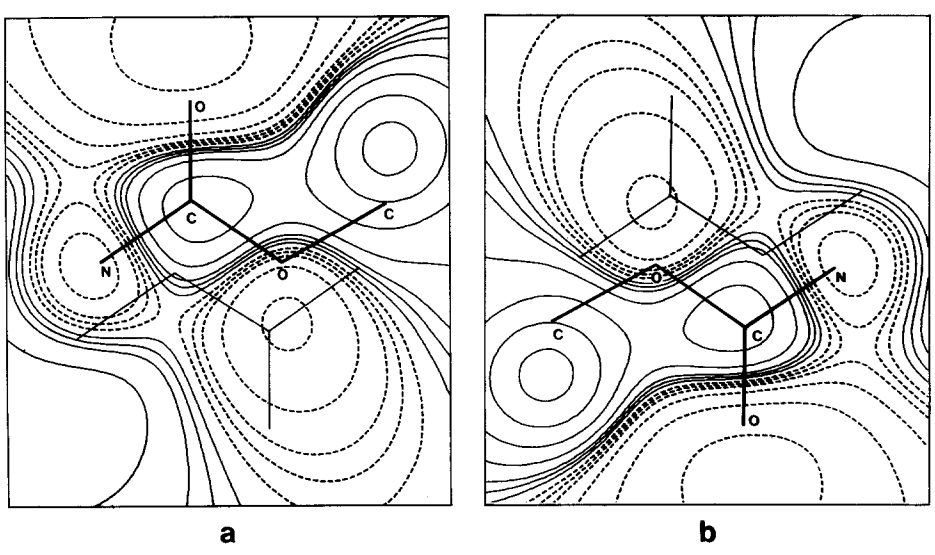


**Fig. 6.** The relative positions of the NCOOC groups in two adjacent layers of the crystal of carbamoylcholine chloride. The layer separation is about 6.5 $a_0$. Features of electrostatic potential approximately midway between the layers and originating from the molecular fragment drawn in heavy line are shown. When (a) and (b) are superimposed it is seen that negative areas originating in one fragment match positive areas from the other. Contours as in Fig. 4

Some crystal packing arrangements, both in the *xy*-plane and between neighbouring layers, may be explained by the electrostatic potentials. Let us compare the structures of carbamoylcholine chloride [7] and methoxycarbonyl choline iodide [8] within the layers. The quaternary ammonium group carries the positive charge on the methyl hydrogens, and it is in both cases surrounded by the same three groups: a halogenide ion, a carbonyl oxygen atom from one molecule and an ester oxygen from another. But in the carbamoylcholine structure the positive ion is found at an angle with respect to the ester oxygen, which matches the area of negative potential, Fig. 5a, whereas the group is symmetrically positioned with respect to the two ester oxygens in methoxycarbonyl choline, Fig. 5b, again in accordance with the electrostatic potential.

If we look at the interactions between molecules in adjacent layers of carbamoylcholine chloride [7], one NCOOC group is placed on top of another, but the sequence is reversed and the units have a relative diplacement of about 1 Å, Fig. 6. Here the negative potential of $O^b$ from one layer matches the positive potential of $C^a$ from the other layer and *vice versa*. Less striking is the complementarity of adjacent layers of methoxycarbonylcholine iodide and of urethane [20]. In these structures the distances between the layers are 3.5 Å and 3.7 Å, respectively, while the interlayer distance in the carbamoylcholine chloride structure is 3.4 Å.

Due to the limitations mentioned above, not all the contacts in the considered crystals can be dealt with in this fashion on basis of the present calculations, but the selected examples demonstrate the kind of information which may be obtained from electrostatic potentials. It is our hope that the potentials in a similar way will contribute to the understanding of the contacts with the active site in acetylcholinesterase and with the different kinds of acetylcholine receptors.

As with the electron densities it is interesting to investigate the changes in potential as a function of R by the use of difference maps. The logarithmic scale in the drawings makes a direct comparison of the potentials difficult. Difference potentials, which $R = CH_3$ as the reference system, have therefore been given in Fig. 7. Due to the long-range nature of the potentials, also the region which contains the substituents has been depicted. The values in the immediate neighbourhood of R are not very meaningful, but the difference at larger distances may be of interest.

It appears that the potential over the $-COOCH_3$ region changes in both of the depicted planes by change of R. Near the carbonyl group the $NH_2$ group gives rise to a decrease in the potential, while the two other substituents have the opposite influence, and an increase in potential is found. This may be correlated to the fact [21] that amides generally have higher affinity for protons and are better acceptors for hydrogen bonds than other classes of carbonyl compounds, while some esters are poorer hydrogen acceptors than ketones, and the same holds to an even greater extent for the fluorine substituted carbonyl compounds. In the region near the ester oxygen atom only $CF_3$ gives rise to a pronounced increase in both of the depicted planes, while the effect of $NH_2$ is a slight increase in the *xz*-plane and a decrease in the plane 3 $a_0$ above, and $OCH_3$ causes a decrease in both of the

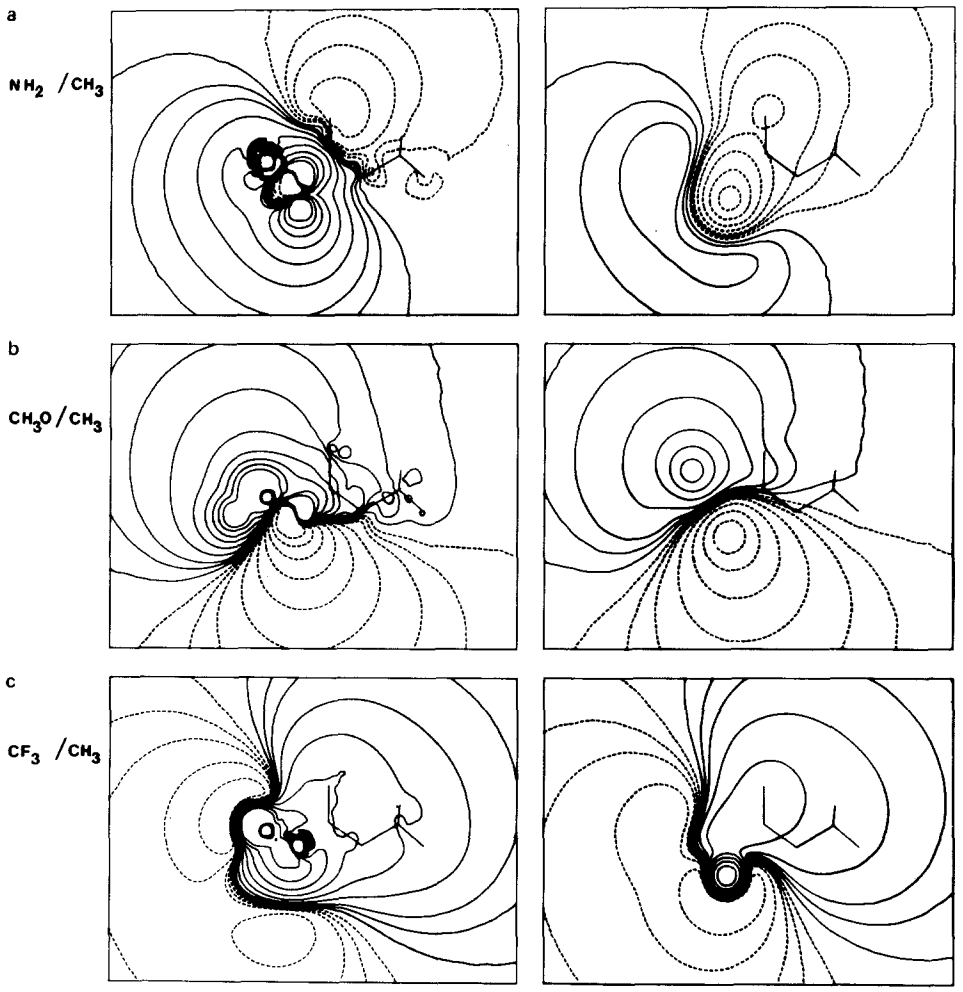


**Fig. 7.** Electrostatic potential differences for systems III to V (Fig. 1) relative to system II. Planes and contours as in Fig. 4

depicted planes. In nearly all of the examined crystal structures of salts of choline esters the torsion angle $OCCN^+$ has been found within the range $\pm 60°$–$\pm 90°$ (called gauche). The approximate position of the quaternary ammonium group relative to the ester group is shown in Fig. 8a and Fig. 8b for molecules with the torsion angle COCC trans and gauche, respectively. There is reason to expect that a decrease of the potential in the surroundings of the ester oxygen atom causes a stabilization of the gauche $OCCN^+$ conformer. It is thus suprising that just carbamoylcholine and methoxycarbonylcholine are the only choline esters, unsubstituted at the methylene groups, which so far have been found to attain the fully extended conformation in crystals. This indicates that intermolecular crystal forces rather than forces within the choline esters may have caused the observed extended conformations.

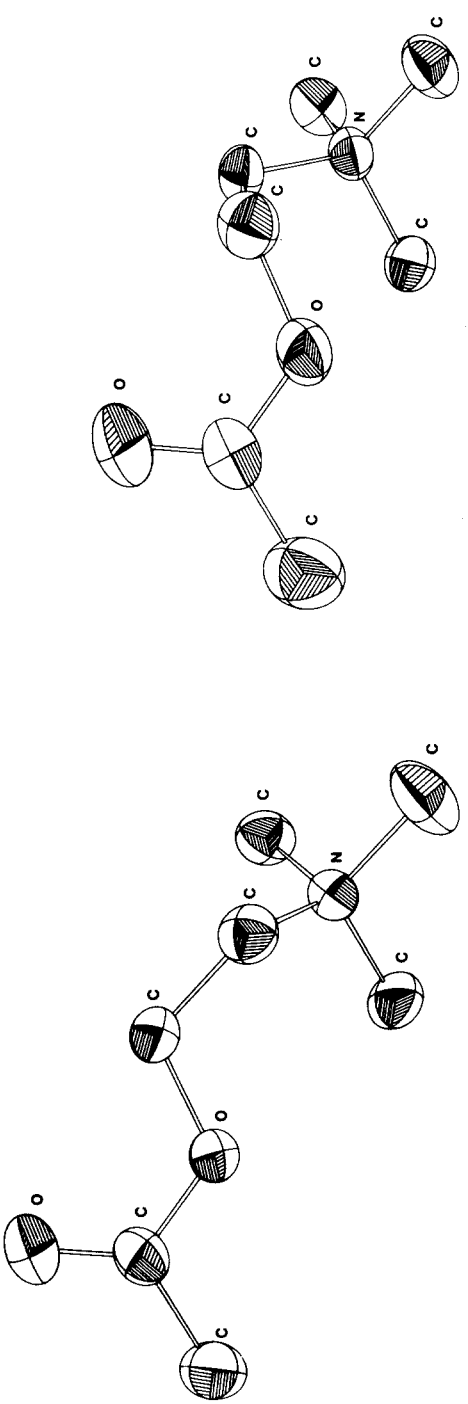


**Fig. 8.** Acetylcholine shown in two characteristic conformations observed in crystal structures. The torsions COCC and OCCN are trans-gauche (a) and gauche-gauche (b). The N-methyl group approaching the ether oxygen atom is $\sim 2\ a_0$ and $\sim 4.5\ a_0$ out of plane in (a) and (b), respectively

The potentials and thereby the contact possibilities in the COOC region of the choline esters are thus affected by the substituent R. Fig. 7b is further dominated by the negative oxygen lone-pair potential of the methoxy oxygen atom and Fig. 7c by the negative regions behind the fluorine atoms.

## 4. Conclusions

In the present investigation a group of related molecules have been compared by means of population analyses, electron density differences, electrostatic potentials, potential differences, and crystal structures. As many parameters as possible were kept constant (basis set and geometry), in order to facilitate comparison and in order to minimize the sources of error. The systems contain many chemically interesting groups, and due to the apparent transferability of many of the considered aspects, the results may be of more general value.

For the choline esters it was concluded that the various substituents give rise to relatively small changes in the electron densities. Some redistribution of electrons between orbitals with $\sigma$ character and orbitals with $\pi$ character was encountered. The electrostatic potentials were found to be significantly different in the region of the ester group. The potentials were further used successfully to explain details in the crystal packing, both within a layer and between layers.

Very little is so far known about the active site of acetylcholinesterase, but it is our hope that the detailed knowledge of the electrostatic potentials for some of the choline esters will contribute to the understanding of the enzyme and the active sites of receptors, and that the present results will be useful in confirming or rejecting possible structures and conformations.

## References

1. Pullman, B.: Adv. Quant. Chem. **10**, 251 (1977)
2. Pullman, A., Port, G. N. J.: Theoret. Chim. Acta (Berl.) **32**, 77 (1973)
3. Port, G. N. J., Pullman, B.: J. Am. Chem. Soc. **95**, 4059 (1973)
4. Weinstein, H., Maayani, S., Srebrenik, S., Cohen, S., Sokolovsky, M.: Molec. Pharmacol. **9**, 820 (1973)
5. Svinning, T., Sørum, H.: Acta Cryst. B **31**, 1581 (1975)
6. Jensen, B.: Acta Chem. Scand. B **30**, 1002 (1976)
7. Jensen, B.: Acta Chem. Scand. B **29**, 891 (1975)
8. Jensen, B.: Acta Chem. Scand. B **33**, 227 (1979)
9. Roothaan, C. C. J.: Rev. Mod. Phys. **23**, 69 (1951)
10. Duijneveldt, F. B. van: IBM Res. Rep. RJ945
11. Roos, B., Siegbahn, P.: Theoret. Chim. Acta (Berl.) **17**, 199 (1970)
12. Almlöf, J.: Proceedings of the Second Seminar on Computational Problems in Quantum Chemistry, Strassburg 1972, pp. 14–25 (Max-Planck-Institut, München 1973)
13. Bagus, P. S.: IBM Res. Rep. RJ1077
14. Mulliken, R. S.: J. Chem. Phys. **23**, 1833 (1955)
15. Del Bene, J. E., Radovick, S.: J. Am. Chem. Soc. **100**, 6936 (1978)
16. Lambrecht, G.: Personal communication
17. Dittert, L. W., Higuchi, T.: J. Pharm. Sci. **52**, 852 (1963)

18. Armstrong, V. C., Farlow, D. W., Moodie, R. B.: J. Chem. Soc. (London) (B) **1968**, 1099
19. Johansen, H.: Acta Cryst. A **35**, 319 (1979)
20. Bracher, B. H., Small, R. W. H.: Acta Cryst. **23**, 410 (1967)
21. Filgueiras, C. A. L., Huheey, J. E.: J. Org. Chem. **41**, 49 (1976)

Received June 25, 1979